

**Thermal, vibrational, structural and optical studies of ZnO and Alkaline Earth Metal (Mg)
doped ZnO Nanoparticles for Antibacterial activity**

M. Sangeetha

*Department of Physics, Auxilium College of Arts and Science for Women (Affiliated to
Bharathidasan University, Trichy), Pudukkottai - 622 302, Tamilnadu, India.*

Author Email id: sangeethadsg@gmail.com; +91-9940945763.

Abstract

Zinc Oxide and Magnesium doped ZnO Nanoparticles (Mg-ZnO NPs) have been synthesized by chemical co-precipitation method and their structural, optical, thermal properties and antibacterial activity have been studied. XRD spectra revealed that all synthesized NPs are hexagonal wurtzite structure and the size of ZnO and Mg-ZnO NPs is 51 and 42 nm. FTIR spectra of ZnO and Mg-ZnO NPs have the peak at 463 and 470 cm^{-1} . Mg-ZnO NPs have enhanced the thermal stability region from (177 - 288 °C) to (198 - 296 °C). ZnO NPs have high antibacterial activity against *Escherichia coli* while Mg-ZnO NPs has the *Pseudomonas aeruginosa*.

Keywords: ZnO; Mg-ZnO; Powder XRD; TGA; Antibacterial activity.

1. Introduction

Semiconductor materials have drawn attention of the scientists for the past years due to their attracting properties such as optical, structural and morphological. The scientific community

treated the ZnO NPs as future material for many optoelectronic applications. Various methods have been used to fabricate ZnO nanoparticles such as vapor-phase growth, vapor liquid solid process, a soft chemical method, electrophoresis deposition, sol gel, homogeneous precipitation, chemical co-precipitation, etc [1]. Among these methods, the chemical co-precipitation is the best low cost method [2] with a high yield rate used for the preparation of large quantity of ZnO and Mg-ZnO NPs. This research focused on their synthesis by chemical co-precipitation method. It is an environmentally friendly material with high chemical stability and low toxicity. They have widely used as the active ingredient for dermatological applications on account of its antibacterial properties [3]. Characteristics of ZnO and Mg-ZnO NPs suitable for biomedical applications demand precise control of particle size, shape and preparation conditions that influence these properties. Different physical or chemical synthetic methods have been used to prepare doped ZnO nanoparticles. To develop the optical absorption properties and attain a small particle size, a search for alternative methods for well-organized Mg-ZnO NPs has become the major interest of study with high surface area for better antibacterial using co-precipitation method [4]. The antibacterial efficiency of ZnO and Mg-ZnO NPs have tested against bacterial growth of *Escherichia coli*, *Pseudomonas aeruginosa*, *Staphylococcus aureus*, *Proteus vulgaris* and *Klebsiella pneumoniae* using disc diffusion method for 24 h. Here, reported that the influences of structural, morphological, vibrational and thermal studies of NPs have also been investigated for their antibacterial activities.

2. Materials and methods

2.1 Materials, Synthesis of ZnO and Mg-ZnO NPs

Zinc chloride, magnesium chloride and sodium hydroxide are purchased from Merck (Mumbai, India). Chemicals were of analytical grade and were used as such. Doubled distilled water

(DDW) was used for preparing solutions. Zinc chloride and sodium hydroxide are dissolved in 100 ml double distilled water separately using magnetic stirrer for 1 h. Then, the sodium hydroxide solution is added drop wise to the zinc chloride solution at room temperature and stirred well. The precipitate was filtered out separately and repeatedly washed with double distilled water to remove unnecessary impurities. Zinc chloride, magnesium chloride and sodium hydroxide are dissolved in 100 ml double distilled water separately as above. Solutions of Zinc Chloride and Magnesium Chloride are mixed together and stirred for about 2 h. Finally, sodium hydroxide solution is added drop wise to this mixture and stirred well. It forms milky white precipitate of Mg-ZnO Nps after 30 minutes continuing the process. It was filtered and dried for further usage [5].

2.2 Characterization techniques and evaluation of antibacterial activities

The available characterization was carried out as per the literature [6]. The prepared ZnO and Mg-ZnO NPs were evaluated the antibacterial studies by disc diffusion method. From this study, antibacterial activity of prepared NPs was analyzed against different bacteria's. An overnight culture of each organism was adjusted to optical density of 0.1 and scrubbed onto Mueller Hilton agar plates. These plates were incubated at 37 °C for 48 h. The inhibition diameter zone was measured in mm scale and its snaps were recorded.

3. Results and Discussion

3.1 Calculation of average crystalline size by XRD spectra

The XRD pattern of synthesized ZnO (a) and Mg-ZnO (b) NPs (Fig. 1) has sharp and highly intense peaks. All the indexed peaks were matched well with JCPDS data (Card Nos.: 36-0451). This was confirmed by the structure of wurtzite hexagonal with lattice parameters ($a = 3.2511\text{\AA}$

and $c = 5.2076\text{\AA}$ for ZnO). In the case of Mg-ZnO, the hexagonal (wurtzite) crystal nature is in also close agreement with the standard values and all the diffraction peak intensity increased due to the effect of higher Mg concentration 10 %. No secondary phases were observed in the samples (for comparison) as showed in Fig. 1a & b which suggested that Mg occupy the zinc sites in the Mg-ZnO NPs. The dominant (101) peak and its higher intensity indicated that the preferential growth of (101) orientation along c-axis for both NPs. Debye-Sherrer's formula [7] was used to calculate the average crystalline size and it was found at 51 and 42 nm for ZnO and Mg-ZnO respectively. XRD results were well correlated with better antibacterial activities in nano-scale.

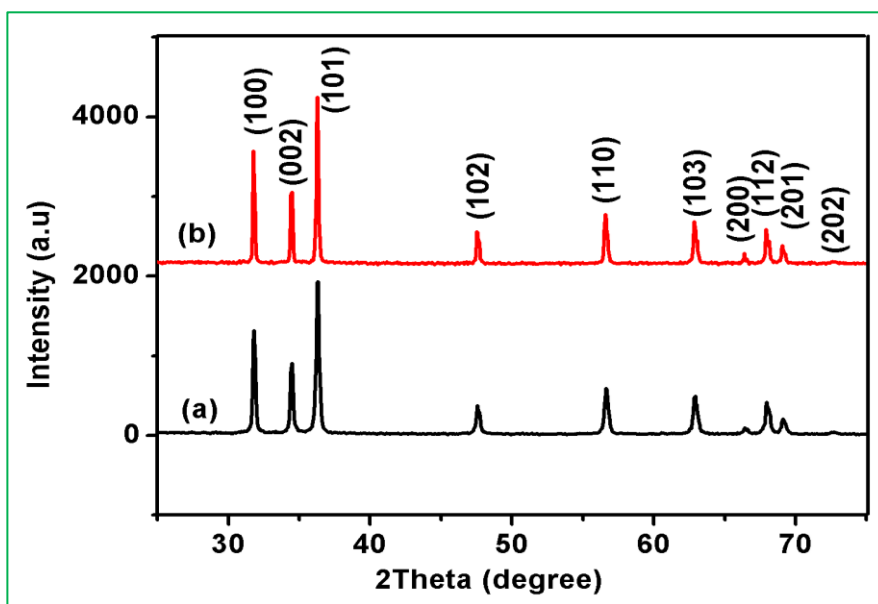


Fig. 1 XRD spectra of synthesized ZnO (a) and Mg-ZnO (b) Nanoparticles for average crystalline size

3.2 Optical and photoluminescence spectra

UV-Vis. Spectra of ZnO (a) and Mg-ZnO (b) NPs (Fig. 2A) showed the absorption peaks at 363 and 367 nm respectively. The small shift in the absorption is attributed to the doping of Mg to

ZnO. The band gaps (E_g) of ZnO and Mg-ZnO NPs were calculated and found as 3.23 and 3.20 eV. PL spectra of ZnO (a) and Mg-ZnO (b) NPs (Fig. 2B) have four main emission bands: a strong UV emission band at ~394 and 384 nm, a weak blue band at ~458 nm, a weak blue-green band at ~490 nm and a very weak green band at ~530 nm. The strong UV emission corresponds to the exciton recombination related to the near-band edge emission of ZnO. Weak blue and weak blue-green emissions are possibly due to surface defects in the NPs. The weak inexperienced band emission corresponds to the separately ionized gas vacancy in ZnO. This emission results from the recombination of a photo-generated hole in the singly ionized charge state of the specific defect. Compared to Mg-ZnO NPs, the low intensity of the green emission of ZnO NPs may be due to the low density of oxygen vacancies when preparation. The strong UV emission intensity should be attributed to the high purity and perfect crystalline of the synthesized nanoparticles [8].

3.3 FTIR spectra

Zn-O bonds were identified at 463 and 846 cm^{-1} which is confirmed the formation of wurtzite structure for the prepared samples. The appearance of band at 1041, 1404 and 15604 cm^{-1} can be attributed to C-O stretching, C=O asymmetric stretching, C=C asymmetric stretching due to Lewis acidity and this C=O symmetric stretching due to Bronsted acidity group those are present in the citrates species on surface of the NPs. For the Mg-ZnO NPs, Zn-O, O-H and C-H bonds have more expanded due to the transformation of hydroxide to alkaline earth metal phase can occur during the process. The results of the present investigation were in good agreement with past reports [9].

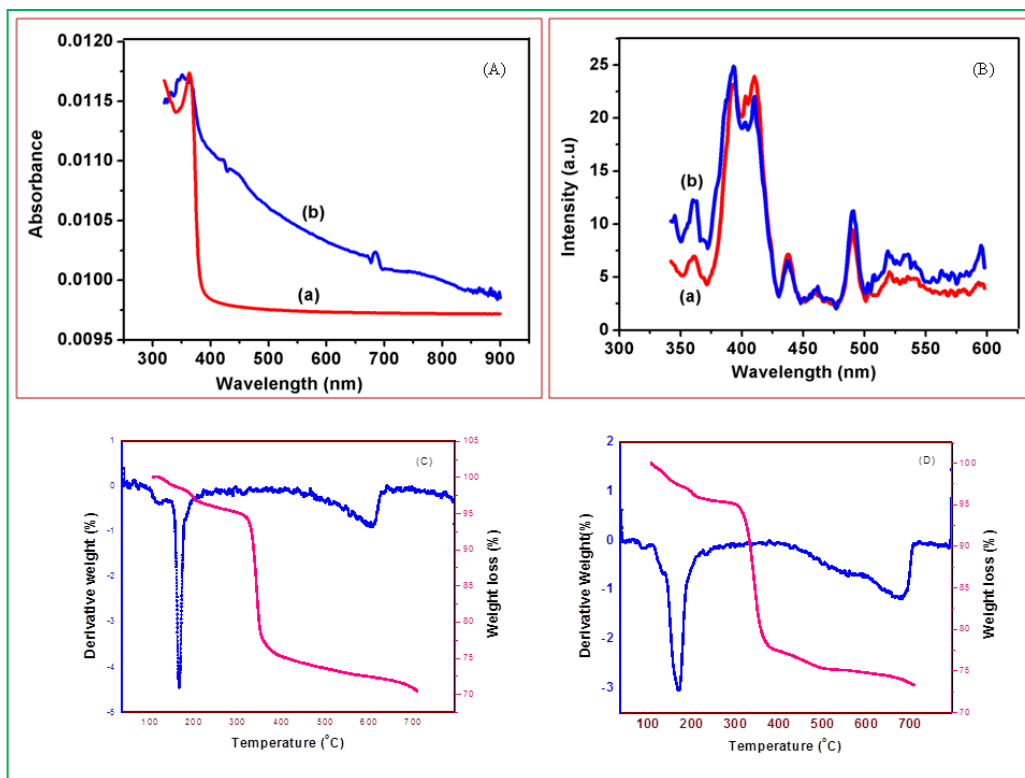


Fig. 2 Optical (A) spectra, PL (B) of synthesized ZnO (a) and Mg-ZnO (b) NPs and TGA/DTA of ZnO (C) and Mg-ZnO (D) NPs.

3.4 Thermal studies

TG/DTA studies of ZnO and Mg-ZnO are shown in Fig. 2C & D. The weight loss of the samples observed at room temperature to 100 °C due to the evaporation of water molecules whereas 100 °C to 400 °C the weight loss caused by evaporation of inorganic materials. After 400 °C, the weight loss occurs due to the evaporation of unreacted materials which is involved in the sample. At 465 °C, the transformation of the hydroxide to oxide is associated with the phase transformation of amorphous ZnO into its cubic ordered phase. From stage I, transition occurs in the temperature range 37-65 °C and 38-98 °C with weight loss of 2 and 2.2 % in the TG thermogram of ZnO and Mg-ZnO NPs respectively. These weight losses are accompanied by 50 °C and 88 °C in DTA curves of ZnO and Mg-ZnO NPs respectively. This transition is attributed

to the evaporation of water molecules. In stage II, transition occurs in the range 100-125 °C and 112-175 °C with weight loss of 2 and 15 % in the TG of ZnO and Mg-ZnO NPs. These weight losses are accompanied by 115 °C and 172 °C in DTA curves of ZnO and Mg-ZnO NPs respectively. In stage III, it occurs in between 146-179 °C and 283-324 °C with weight loss of 18 and 2 % in TGA and their weight losses are accompanied by 116 °C and 235 °C in DTA. The IV stage transition occurs in the ranges 576-617 °C and 379-436 °C with weight loss of 2 and 2.2 % in TGA. These weight losses are accompanied by 604 °C and 400 °C in DTA curves of ZnO and Mg-ZnO. Finally, stage V transition occurs in the range 540-652 °C with weight loss of 17% in the TG of Mg-ZnO NPs. These weight losses are accompanied by 688 °C in DTA curves of Mg-ZnO NPs. This transition is attributed to evaporation of entire water molecules. The stable regions of ZnO NPs are enhanced by the ranges (177-288 °C) while Mg-ZnO (198-296 °C) [10].

3.5 Antibacterial activities of ZnO and Mg-ZnO NPs

The antibacterial efficiency of ZnO and Mg-ZnO (Fig. 3) NPs tested by disc diffusion method for 48 h against five different pathogenic bacteria's *Escherichia coli*, *Pseudomonas aeruginosa*, *Staphylococcus aureus*, *Proteus vulgaris* and *Klebsiella pneumoniae*. From the results revealed that, ZnO NPs have high antibacterial activity against *Escherichia coli* while Mg-ZnO NPs affects on the *Pseudomonas aeruginosa*.

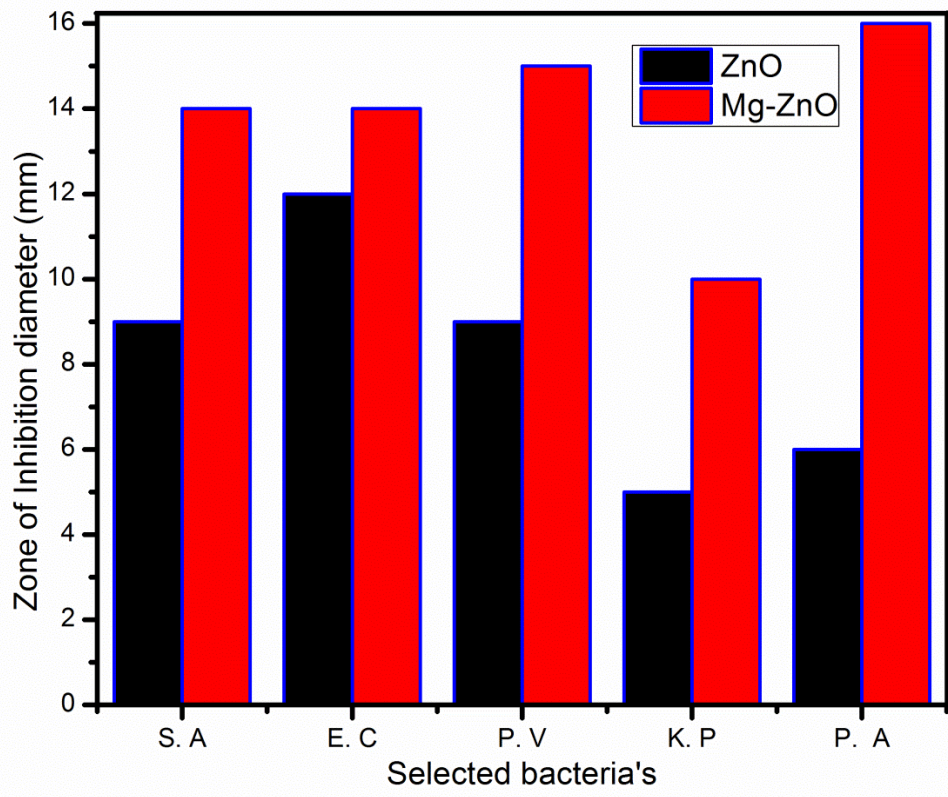


Fig. 3 Antibacterial activities of synthesized ZnO (a) and Mg-ZnO (b) Nanoparticles

4. Conclusion

Alkaline earth materials of Mg-ZnO and ZnO NPs were successfully synthesized and prepared. Mg-ZnO NPs have enhanced the thermal stability region from (177 - 288 °C) to (198 - 296 °C). Antibacterial efficiency was affected by size and optical properties for the influence Mg-ZnO. It was noted that, ZnO NPs have high antibacterial activity against *Escherichia coli* while Mg-ZnO NPs effects on the *Pseudomonas aeruginosa*. Due to intense antibacterial properties of ZnO and Mg-ZnO NPs against some bacteria's addressed in pharmaceutical, water purification and preservative system with non-toxic.

References

- [1] K. Pradeev raj, K. Sadaiyandi, A. Kennedy, S. Sagadevan, Z. Chowdhury, M. R. Johan, F. A. Aziz, R. F. Rafique, R. Thamiz Selvi, R. Rathina bala, *Nanoscale Res. Lett.* 229 (2018) 1-13.
- [2] A. Jafar Ahamed, P. Vijaya Kumar, M. Karthikeyan, *J. Environ. Nanotechnol.* 5 (2016) 11-16.
- [3] W. Zhang, G. Tu, H. Zhang, Y. Zheng, L. Yang, *Mater. Lett.* 114 (2014) 119-121.
- [4] M. Ramani, S. Ponnusamy, C. Muthamizhchelvan, J. Cullen, S. Krishnamurthy, E. Marsili, *Col. Surf. B: Biointer.* 105 (2013) 24-30.
- [5] A. Dhanalakshmi, A. Palanimurugan, B. Natarajan, *Carb. Pol.* 168 (2017) 191-200.
- [6] A. Dhanalakshmi, A. Palanimurugan, B. Natarajan, *Mat. Sci. Engg. C.* 90 (2018) 95-103.
- [7] H. H. Choi, M. Ollinger, R. K. Singh, *Appl. Phys. Lett.* 82 (2003) 2494-2496.
- [8] V. Senthamilselvi, K. Saravanakumar, N. Jabena Begum, R. Anandhi, A. T. Ravichandran, B. Sakthivel, K. Ravichandran, *J. Mater. Sci: Mater. Electron.* 23 (2012) 302-308.
- [9] J. Fang, H. Nakamura, H. Maeda, *Adv. Drug Deliv. Rev.* 63 (2011) 136-151.
- [10] A. Palanimurugan, A. Kulandaisamy, *J. Organ. Chem.* 861 (2018) 263-274.